J Appl Electrochem (2010) 40:1859–1865
DOI 10.1007/s10800-010-0107-9

ORIGINAL PAPER

The role of TiO_2 layers deposited on YSZ on the electrochemical promotion of C_2H_4 oxidation on Pt

E. I. Papaioannou · S. Souentie · F. M. Sapountzi · A. Hammad · D. Labou · S. Brosda · C. G. Vayenas

Received: 22 January 2010 / Accepted: 18 February 2010 / Published online: 12 March 2010

Abstract The electrochemical promotion of Pt/YSZ and Pt/TiO_2/YSZ catalyst-electrodes has been investigated for the model reaction of C_2H_4 oxidation in an atmospheric pressure single chamber reactor, under oxygen excess between 280 and 375 °C. It has been found that the presence of a dispersed TiO_2 thin layer between the catalyst electrode and the solid electrolyte (YSZ), results in a significant increase of the magnitude of the electrochemical promotion of catalysis (EPOC) effect. The rate enhancement ratio upon current application and the faradaic efficiency values, were found to be a factor of 2.5 and 4 respectively, higher than those in absence of TiO_2. This significantly enhanced EPOC effect via the addition of TiO_2 suggests that the presence of the porous TiO_2 layer enhances the transport of promoting O^{2-} species onto the Pt catalyst surface. This enhancement may be partly due to morphological factors, such as increased Pt dispersion and three-phase-boundary length in presence of the TiO_2 porous layer, but appears to be mainly caused by the mixed ionic-electronic conductivity of the TiO_2 layer which results to enhanced O^{2-} transport to the Pt surface via a self-driven electrochemical promotion O^{2-} transport mechanism.

Keywords TiO_2 interlayer · EPOC · NEMCA effect · Sputtered Pt electrodes · C_2H_4 oxidation

E. I. Papaioannou · S. Souentie · F. M. Sapountzi · A. Hammad · S. Brosda · C. G. Vayenas (✉)
LCEP, Department of Chemical Engineering, University of Patras, 26500 Patras, Greece
e-mail: cgvayenas@upatras.gr

D. Labou
Institute of Chemical Engineering and High Temperature Chemical Processes, 26504 Rio, Patras, Greece

1 Introduction

Titania is an important support material both from a practical and a fundamental point of view and has been studied extensively in the context of metal-support interactions (MSI) and in particular that of strong metal-support interactions (SMSI) [1–10]. The origin of the classical SMSI effect has been shown to be metal decoration by TiO_x moieties [2–5]. In addition titania is a very significant material in sensor technology [11] due to its semiconductivity type dependence on oxygen concentration and the marked variation in its electronic conductivity with oxygen chemical potential. Also, titania has been extensively studied in photocatalysis for photocatalytic purifiers [12, 13] and photochemical solar cells [14, 15].

A variety of techniques are used for the preparation of titania thin films, such as sol–gel processes [16], chemical vapour deposition [17, 18] and evaporation [19]. However, the technique of sputtering is more widely used in industrial processes, since high-density homogenous films can be prepared at low temperatures.

The electrochemical promotion of catalysis (EPOC) or non-Faradaic electrochemical modification of catalytic activity (NEMCA) is a phenomenon where the application of a small current or potential between a catalyst-electrode which is in contact with a solid electrolyte support and a counter electrode causes significant changes in the catalytic activity and selectivity of the catalytic reaction. The EPOC effect has been investigated extensively for more than seventy catalytic systems using a variety of catalytic reactions and metal or metal oxide catalysts [20, 21]. It has been found using numerous electrochemical and surface science techniques [20, 21] that EPOC originates from the electrochemically controlled backspillover of ionic promoting species (O^{2-} in case of YSZ and TiO_2) which migrate from

the electrolyte support to the metal/gas interface during polarization [20, 21]. Two parameters are commonly used to quantify the magnitude of the EPOC effect:

1. the rate enhancement ratio, ρ, defined from:

$$\rho = r/r_o \quad (1)$$

where r is the electropromoted catalytic rate and r_o the normal, open-circuit catalytic rate.

2. the apparent faradaic efficiency, Λ, defined from:

$$\Lambda = (r - r_o)/(I/nF) \quad (2)$$

where I is the applied current, F the Faraday's constant and n is the charge of the ionic species (n = 2 for O^{2-}), thus I/nF equals the rate of ionic species supplied to the catalyst.

A reaction exhibits electrochemical promotion when $|\Lambda| > 1$, while electrocatalysis is limited to $|\Lambda| \leq 1$. Typical $|\Lambda|$ values from 10 to 10^5 have been recorded depending on the reaction, the catalyst material and morphology, the type of solid electrolyte support and the operating temperature [20–33]. A reaction is termed electrophobic when $\Lambda > 1$ and electrophilic when $\Lambda < -1$. In the former case the rate increases with increasing catalyst potential, U, while in the latter case the rate decreases with increasing catalyst potential.

Titania, without any YSZ support, has already been used under oxidizing conditions as a mixed electronic-ionic (O^{2-}) support to reversibly enhance the catalytic activity of Pt for the C_2H_4 oxidation reaction, where a 20-fold increase of the rate was recorded with apparent faradaic efficiency reaching 2000 [9]. The use of titania as a dispersed thin interlayer between Rh catalyst electrodes and a solid electrolyte (YSZ) support, was first pioneered by Baranova, Foti and Comninellis for the case of Rh catalyst-electrodes [34–36]. These and subsequent studies [37, 38] showed that the presence of the porous TiO_2 layer enhances the open-circuit catalytic rate for CH_4 and C_2H_4 oxidation on Rh and also stabilizes the electrochemically promoted highly active Rh catalyst state. This pronounced effect was attributed to a self-driven wireless-EPOC mechanism, where O^{2-} promoting species are supplied from TiO_2 to Rh particles due to TiO_2-Rh work function difference and the subsequent charge transfer from TiO_2 to Rh via a self driven EPOC O^{2-} transport mechanism [34–36]. More recently it was found that the presence of a thin TiO_2 layer deposited on YSZ also enhances the electropromotion of CO_2 hydrogenation over Cu/TiO_2/YSZ catalyst electrodes under reducing conditions [39]. In this case the enhanced electropromotion was attributed to the electronic conductivity of the TiO_2 layer which decreases the in-plane resistance of the porous Cu catalyst-electrode [39].

In the present study, the effect of TiO_2 interlayer was examined on the catalytic activity and EPOC behavior of C_2H_4 oxidation on Pt by comparing a Pt/YSZ catalyst electrode and a Pt/TiO_2/YSZ catalyst electrode under similar operating conditions in excess O_2.

2 Experimental

2.1 Sample preparation

The solid electrolyte was a disk of 8 mol% Y_2O_3-stabilized ZrO_2 (YSZ) of 18 mm diameter and 2 mm thickness. Gold counter and reference electrodes were deposited on one side of the disk by applying thin coatings of Engelhard 8300 Au paste, followed by calcination in air for 90 min at 400 °C and for 30 min at 650 °C. The Pt catalyst film was deposited on the other side of the disk, opposite to the counter electrode, serving also as the working electrode.

Two types of catalyst-electrodes were prepared: Pt/YSZ and Pt/TiO_2/YSZ. The Pt and TiO_2 thin films were prepared using a magnetron sputtering system. High purity argon and oxygen have been used as sputtering and reactive gas, respectively. The discharge characteristics have been controlled using a variable DC power supply (1 kV and 2 A). Pure Ti (99.95%) and Pt (99.95%) have been used as sputtering targets.

For the preparation of the Pt/TiO_2/YSZ catalyst-electrode, initially a thin (90 nm) TiO_2 film was sputter-deposited on the area of the working electrode on the YSZ disk, with 600 W target power, which enables 0.5 nm min^{-1} deposition rate (of TiO_2) and leads to a 90 nm film thickness after 180 min of deposition. The substrate temperature was kept stable during the deposition at 250 °C. Also, a post-deposition annealing of the deposited TiO_2 film was performed in air at 600 °C for 60 min.

The Pt films were sputter deposited over the YSZ disk for the Pt/YSZ catalyst-electrode and over the above mentioned TiO_2 thin layer on the YSZ disk for the Pt/TiO_2/YSZ catalyst electrode. The target power was kept constant at 190 W, which led to a 18 nm min^{-1} deposition rate and to a 30 nm thick Pt film after 1.5 min in both samples. The substrate temperature was kept stable at 50 °C. During all depositions the substrates were placed 55 cm far from the target which was found to result in good uniformity of the produced films.

2.2 Catalyst characterization

The surface characterization of the TiO_2 sputtered films was carried out using X-ray photoelectron spectroscopy (XPS). The spectra of Ti 2p and O 1s are shown in Fig. 1a. Correcting the energy scale using the C 1s peak at 284.6 eV as an intrinsic reference, the position of the Ti $2p_{3/2}$ and O 1s peaks is estimated at 458 ± 0.2 and

529 ± 0.2 eV respectively and indicates the presence of TiO_2 [40–42]. The atomic ratio of Ti:O = 1:3 was found by means of XPS analysis, reflecting the enrichment of the surface with hydroxyl species which are physically adsorbed thus do not affect its chemical state [43].

The diffractogram (XRD) obtained from the titanium dioxide layer deposited over the YSZ substrate is shown in Fig. 1b. Scans were collected in the range of 2θ between 10 and 70° with a scanning rate of 0.02°/s and the crystal planes of the deposited films where identified according to JCPDS crystallographic data base. It is observed that the TiO_2 layer is in its anatase (JCPDS file No 21-1272) and rutile (JCPDS file No 21-1276) form. The ratio (x_A) of anatase in the TiO_2 sample was ca. 38% using [44]:

$$x_A = [1 + 1.26(I_R/I_A)]^{-1} \quad (3)$$

where I_A and I_R are the integral intensities of the anatase and rutile reflections of the primary peaks, respectively.

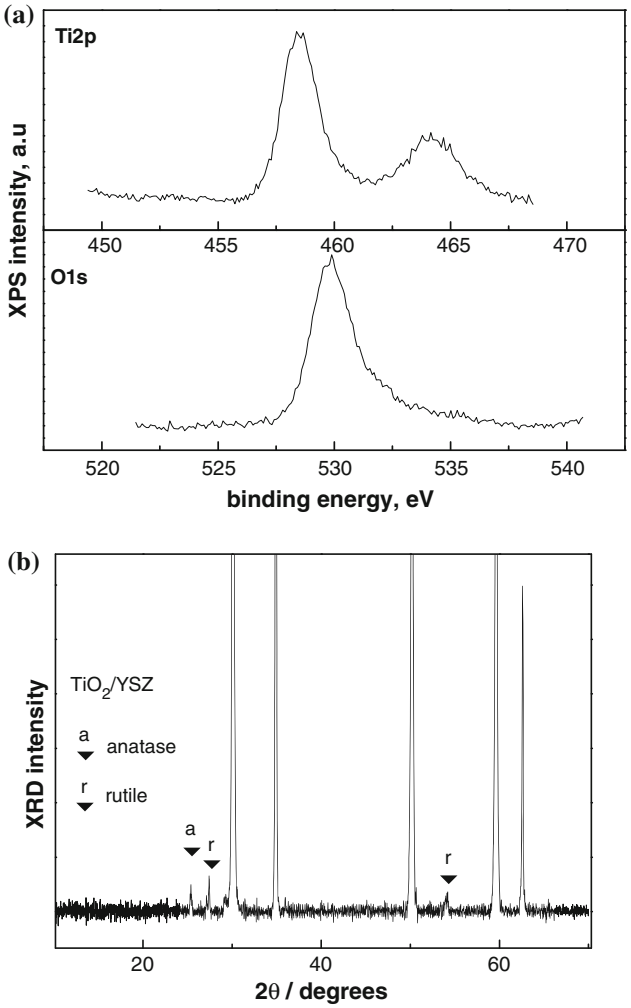

Fig. 1 Surface characterisation: **a** XPS spectra of the TiO_2 interlayer and **b** XRD spectra of TiO_2/YSZ support

The secondary reflections of TiO_2 crystal forms are hidden by the YSZ spectra.

The surface morphology of the solid electrolyte support and of the deposited films was examined using Scanning Electron Microscopy (SEM). Figure 2a presents a SEM micrograph of the YSZ substrate while Fig. 2b shows the TiO_2/YSZ surface before the deposition of Pt. Worth to note is that the YSZ substrate is not fully covered by the TiO_2 thin layer. Figure 2c presents a SEM micrograph of the Pt/TiO_2/YSZ catalyst-electrode surface. As shown, the Pt layer exhibits a high roughness morphology.

The catalytically active surface area of the Pt catalytic films can be estimated using the galvanostatic transient technique, by measuring the time, τ, required for the rate increase, Δr, in galvanostatic electropromotion rate transients to reach 63% of its steady-state value [21]. In this way one can estimate the reactive oxygen uptake, N_G, of the anodically polarized metal film and, assuming a 1:1 surface metal:O ratio, the catalyst active surface area, N_G, expressed in mol Pt, is calculated from:

$$N_G = I\tau/(2F) \quad (4)$$

during current imposition [20, 21] or from:

$$N_G = r\tau_D/\Lambda \quad (5)$$

in the current interruption technique [20, 21], where r is the electropromoted rate while the depolarization time, τ_D, expresses the mean lifetime of the backspillover oxygen species on the catalyst surface and is extracted from the rate transient upon current interruption [20, 21]. These promoting O^{2-} species are more strongly bonded to the catalytic surface than normally adsorbed oxygen from the gas phase [20, 21].

When thin (<1 μm) Pt films are used at high (>300 °C) operating temperatures the effect of thermally migrated promoting species on the initial open-circuit rate is significant and thus Eq. 4 leads to overestimated N_G values [20, 33]. In this case, the current interruption technique (Eq. 5) which is not directly linked to the open-circuit coverage of the promoting O^{2-} species, results in more accurate values of the active surface area. Thus using Eq. 5, the active surface area of the Pt/YSZ and Pt/TiO_2/YSZ catalyst-electrodes was estimated to be 1.7×10^{-8} and 4.7×10^{-8} mol Pt, respectively. This increased Pt surface area in presence of the TiO_2 layer is in qualitative agreement with the Atomic Force Microscopy (AFM) analysis, where ~50% higher roughness of the substrate surface has been found in presence of the TiO_2 layer.

2.3 Reactor operation

The apparatus utilizing on-line gas chromatography (Shimadzu GC-14A, equipped with a TC detector and a

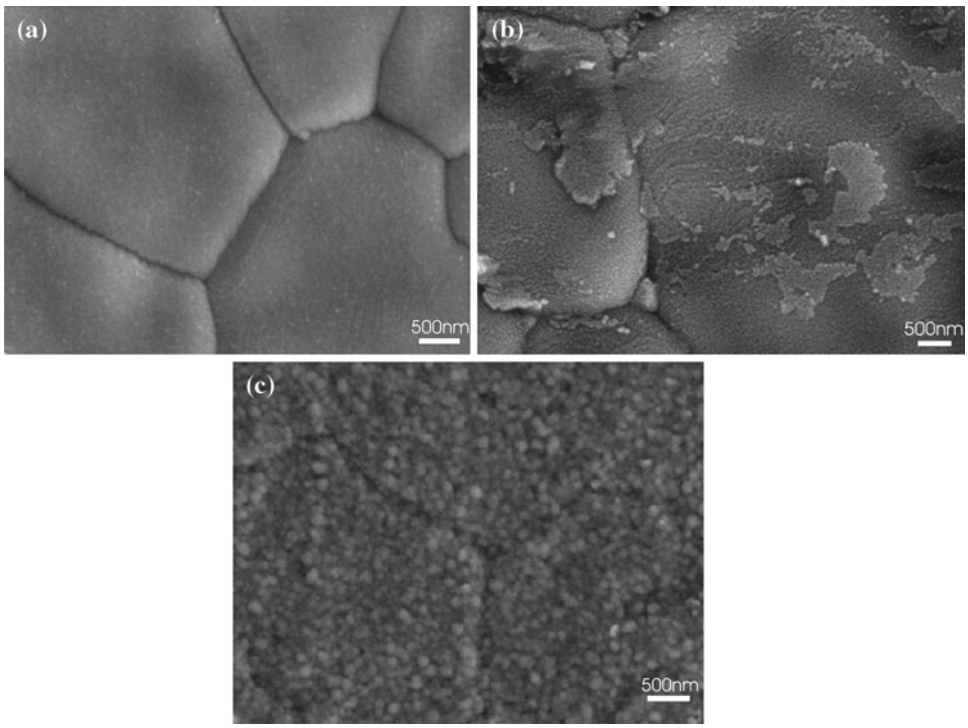

Fig. 2 SEM micrograph top views of **a** the YSZ surface, **b** the TiO_2/YSZ surface before the deposition of Pt and **c** the Pt/TiO_2/YSZ. Magnification factor of 5000 (scale markers of 500 nm)

Porapaq-N 80/100 packed column, for the C_xH_y analysis), and IR spectroscopy (Fuji electric, for the CO_2 analysis) has been described previously [9, 37]. Reactants were Messer Griesheim-certified standards of C_2H_4 in He and O_2 in He and could be further diluted in (99.999%) He (L'Air Liquide). The atmospheric pressure single chamber quartz reactor has a volume of 30 cm^3 and has been previously described in detail [9, 20, 21, 37]. The C_2H_4 and O_2 partial pressures in the feed were held constant during all the experiments at 0.19 and 8.2 kPa, respectively. The gas flow was regulated by Brooks mass flow controllers connected to a four-channel Brose control box (model 5878). The total gas flow was 420 cm^3 (STP) min^{-1}. Constant currents or potentials were applied using an AMEL 2053 galvanostat-potentiostat.

3 Results

Figure 3 compares the transient and steady-state electrochemical promotion of the Pt/YSZ and Pt/TiO_2/YSZ catalysts at 280 °C and inlet $p_{C_2H_4}$ and p_{O_2} values of 0.19 and 8.2 kPa respectively by examining two galvanostatic transients.

Thus Fig. 3a shows the transient effect of constant current application and interruption on the rate of C_2H_4 oxidation and corresponding C_2H_4 conversion and on the catalyst potential U_{WR} relative to the reference electrode for the Pt/YSZ catalyst. Figure 3b shows the corresponding transients for the Pt/TiO_2/YSZ catalyst.

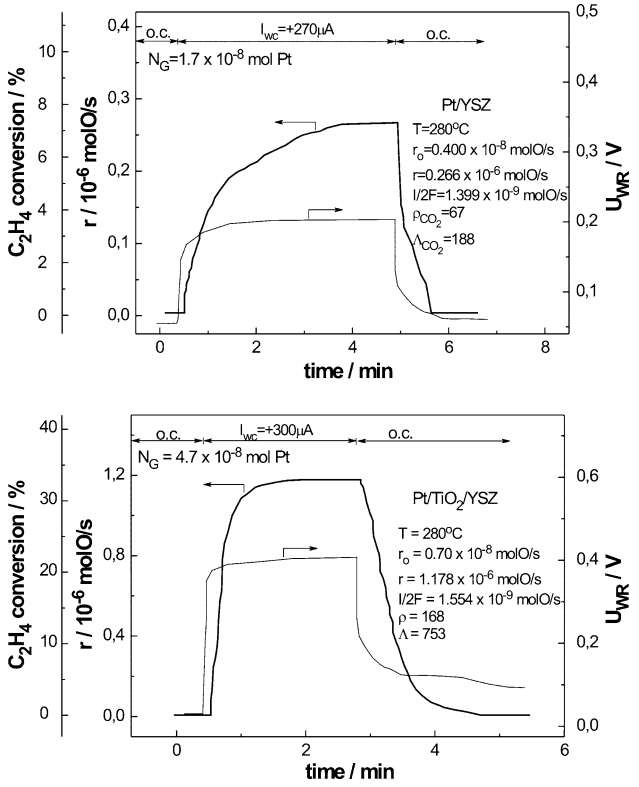

Fig. 3 Transient effect of applied constant current on the rate of C_2H_4 oxidation (expressed in mol O/s), on C_2H_4 conversion and on the working-reference potential difference. (*top*): Pt/YSZ catalyst; (*bottom*): Pt/TiO_2/YSZ catalyst. T = 280 °C, p_{O_2} = 8.2 kPa, $p_{C_2H_4}$ = 0.19 kPa

In both cases significant and reversible electropromotion occurs with the rate enhancement ratio ρ reaching values of 67 for the Pt/YSZ catalyst and 168 for the Pt/TiO_2/YSZ catalyst (i.e. 16700% rate increase).

The corresponding Faradaic efficiency Λ values are 188 for the Pt/YSZ catalyst and 753 for the Pt/TiO_2/YSZ catalyst. Thus in the latter case each O^{2-} ion supplied to the Pt catalyst causes on the average the catalytic reaction of 753 adsorbed O species originating from the gas phase.

Thus the electropromotion of the Pt/TiO_2/YSZ catalyst is significantly more pronounced than the electropromotion of the Pt/YSZ catalyst since the ρ and Λ values are a factor of 2.5 and 4 higher, respectively.

There are three additional useful observations made by comparing Fig. 3a and b:

a. The increase in U_{WR} for the case of the Pt/TiO_2/YSZ catalyst ($\Delta U_{WR} = 590$ mV) is significantly higher than that ($\Delta U_{WR} = 340$ mV) for the Pt/YSZ catalyst. Since it is well established that over wide range of experimental conditions it is [20, 22, 28]:

$$e\Delta U_{WR} = \Delta\Phi \quad (6)$$

this implies that the increase in the work function, Φ, of the Pt catalyst is significantly higher in the case of the Pt/TiO_2/YSZ catalyst which in turn implies a higher coverage of promoting spillover O^{2-} species on the catalyst surface.

b. The approach to steady state upon positive current application is significantly faster in the case of the Pt/TiO_2/YSZ catalyst.

c. Although the open circuit catalytic rate, r_o, is higher for the case of the Pt/TiO_2/YSZ catalyst ($r_o = 0.70 \times 10^{-8}$ mol O/s vs $r_o = 0.40 \times 10^{-8}$ mol O/s the corresponding open-circuit turnover frequencies (TOFs) are similar (TOF = 0.15 s^{-1} vs TOF = 0.23 s^{-1}). Thus although the presence of the TiO_2 layer enhances N_G (by a factor of 2.8) and thus enhances the dispersion of Pt, there appears to be no beneficial effect on the specific catalytic activity or turnover frequency.

The above observations a and b show that the presence of the TiO_2 layer, which according to observation c does not affect significantly the open-circuit TOF, enhances significantly the supply of the promoting O^{2-} species onto the catalyst surface upon anodic polarization, i.e. upon imposition of positive current. This TiO_2-assisted enhanced O^{2-} supply to the catalyst surface is similar to that observed for Rh/TiO_2/YSZ catalysts [34–38] and the underlying mechanism based on the mechanisms of SMSI and of the EPOC theory has been discussed in detail by Baranova, Foti and Comninellis [34] as outlined in Discussion.

Figures 4 and 5 present steady state results of the effect of the IR-corrected potential U_{WR} on current (open symbols) and on the catalytic rate (and corresponding conversion and TOF) for the Pt/YSZ and Pt/TiO_2/YSZ catalysts first at T = 280 °C (Fig. 4) and then at 375 °C (Fig. 5).

One observes in Fig. 4 that the presence of the TiO_2 layer enhances the maximum ρ value obtained at high anodic polarization. The presence of the TiO_2 layer also significantly increases the anodic current and appears to also decrease by almost 300 mV the onset potential for rate enhancement upon anodic ($U_{WR} > 0$) polarization. Both in presence and absence of the TiO_2 layer purely electrophobic behaviour is observed.

At higher temperatures (T = 375 °C, Fig. 5) the r vs U_{WR} behaviour shifts from purely electrophobic to inverted volcano in accordance to the rules of chemical and electrochemical promotion [20]. Physically this reflects the decrease in the coverage of the reactants, more notably atomic oxygen, on the Pt catalyst surface with increasing temperature. Interestingly at 375° the open circuit catalytic rates is lower for the Pt/TiO_2/YSZ catalyst but this catalyst again exhibits the highest anodically electropromoted rate. Interestingly the Pt/YSZ catalyst exhibits higher cathodically $U_{WR} < 0$ electropromoted rate.

Figure 6 shows the steady state effect of current, or equivalently rate of O^{2-} supply or removal, to the catalyst surface on the rate increase Δr during C_2H_4 oxidation on Pt/YSZ and Pt/TiO_2/YSZ at 280 °C (Fig. 6a) and at 375 °C (Fig. 6b). According to the definition of Λ (Eq. 2), straight lines passing from the origin are constant faradaic

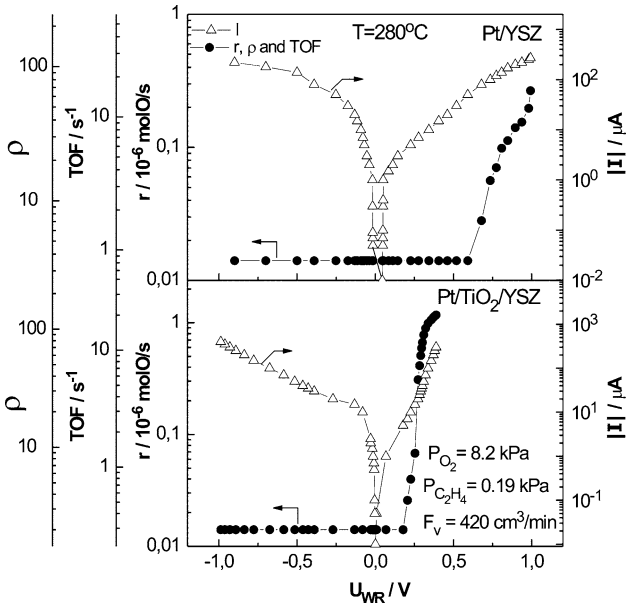

Fig. 4 Steady-state effect of catalyst potential on the rate of C_2H_4 oxidation, on turnover frequency (TOF), on rate enhancement ratio (ρ) and on the current (I) for the Pt/YSZ and Pt/TiO_2/YSZ catalysts at 280 °C

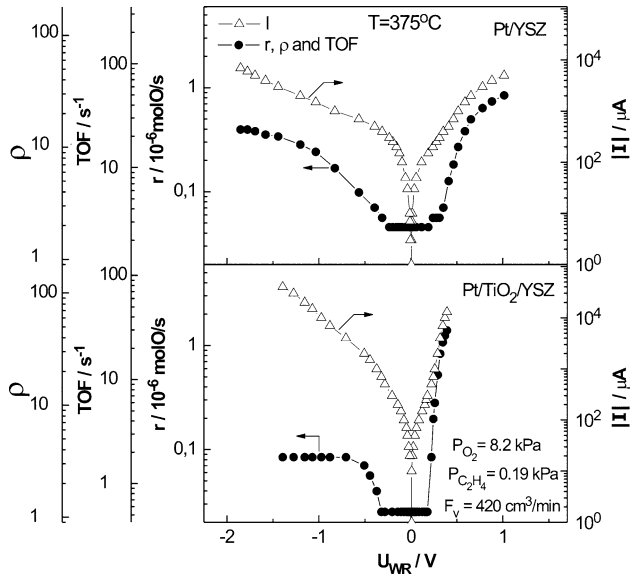

Fig. 5 Steady-state effect of catalyst potential on the rate of C_2H_4 oxidation, on turnover frequency (TOF), rate enhancement ratio (ρ) and on the current (I) for the Pt/YSZ and Pt/TiO_2/YSZ catalysts at 375 °C

efficiency lines. As shown in Fig. 6a, low I/2F values lead to Λ values up to 4000 for the Pt/TiO_2/YSZ catalyst and up to 180 for the Pt/YSZ catalyst. This implies that each O^{2-} supplied to the catalyst causes the reaction of up to 4000 oxygen atoms adsorbed from the gas phase. At higher temperatures (Fig. 6b), the Λ values decrease for both catalysts in agreement with all previous EPOC studies [20].

4 Discussion

The enhancement of EPOC efficiency of Pt via the addition of the TiO_2 sublayer can be interpreted by the enhanced O^{2-} transport to the Pt catalyst surface resulting from self-driven wireless EPOC where O^{2-} species are provided from the TiO_2 to the Pt surface, as first proposed by Baranova, Foti and Comninellis [34, 35] (Fig. 7).

In this mechanism the occurance of the catalytic reaction on the Pt catalyst surface upon anodic polarization and concomitant slow consumption of the promoting spillover O^{2-} species on the same surface causes a decrease in the oxygen chemical potential on the Pt/gas and Pt/TiO_2 interfaces and thus a local gradient in the oxygen chemical potential between these interfaces and regions of higher oxygen chemical potential, e.g. at the TiO_2/gas or TiO_2/YSZ or even conceivably at the TiO_x/gas interface where O_2 reduction may also take place (Fig. 7). Due to the mixed ionic (O^{2-}) and electronic conductivity of the TiO_2 layer this gradient can cause migration of promoting O^{2-} species from the TiO_2/gas interface to the Pt/gas interface

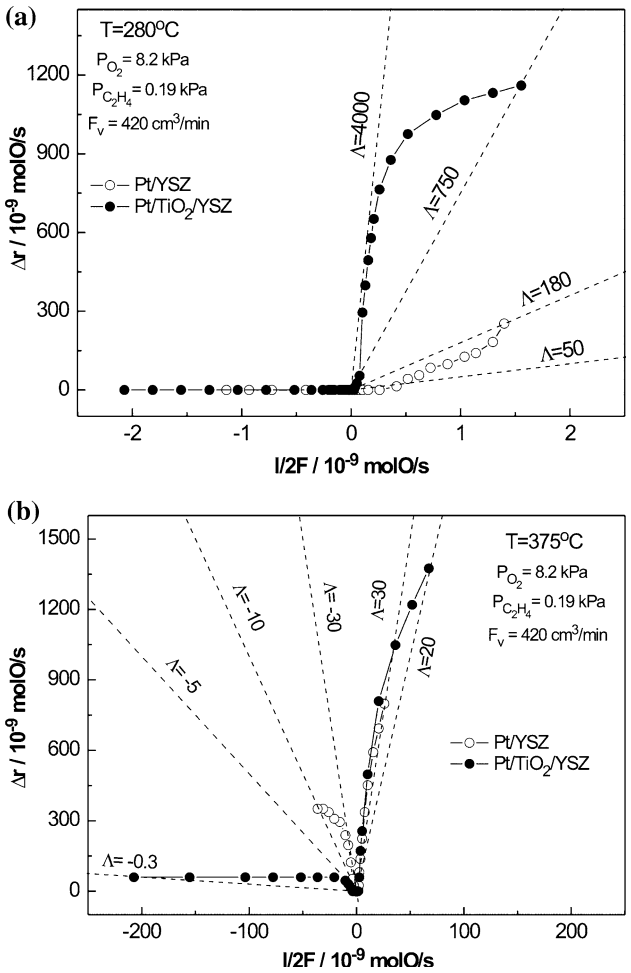

Fig. 6 Effect of O^{2-} supply rate (or removal) to (or from) the catalyst electrode on the increase in the rate of C_2H_4 oxidation on the Pt/YSZ (*open symbols*) and Pt/TiO_2/YSZ (*filled symbols*) catalysts at 280 °C (*top*) and 375 °C (*bottom*). *Dashed lines* are constant faradaic efficiency, Λ, *lines*

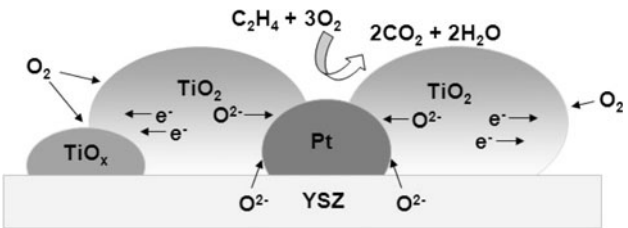

Fig. 7 Schematic of the self driven enhanced O^{2-} transport electrochemical promotion mechanism of C_2H_4 oxidation on Pt interfaced with TiO_2 with internal short-circuiting. Adapted from Fig. 7 in [34]

via the TiO_2 layer, thus establishing a self-driven EPOC mechanism [20, 34, 35]. In this way the TiO_2 layer under polarization acts as a catalyst for transforming gaseous O_2 to promoting O^{2-} species at the Pt/gas interface.

This gradient in the oxygen chemical potential is expected to be negligible under open-circuit conditions,

since in this case the catalytic rate on the Pt surface is much smaller. This can explain why this self-driven enhanced O^{2-} transport mechanism manifests itself only upon anodic polarization and not under open-circuit conditions where the TiO_2 layer has no promoting effect on the catalytic rate.

In summary the presence of such thin TiO_2 layers between the catalyst and the solid electrolyte enhances very significantly the EPOC behaviour of both Rh and Pt catalysts under anodic polarization conditions. The exact mechanism is certainly worth further investigation via oxygen isotopic and surface spectroscopic technique.

5 Conclusions

The catalytic and electrocatalytic activity of Pt/YSZ and Pt/TiO_2/YSZ electrodes has been investigated for the model reaction of C_2H_4 oxidation in an atmospheric pressure single chamber reactor, in excess oxygen at 280 and 375 °C. It has been found that the presence of the dispersed TiO_2 interlayer results in a very significant increase in the magnitude of the electrochemical promotion effect upon anodic polarization. The rate enhancement ratio and the apparent faradaic efficiency values were found to be a factor of 2.5 and 4, respectively, higher than in absence of the TiO_2 interlayer. This significant enhancement in EPOC efficiency is similar to that previously observed for Rh catalysts and appears to be mainly due to enhanced transport of promoting O^{2-} species onto the metal catalyst surface under anodic polarization conditions. This is corroborated both by the faster galvanostatic transients and by the increased catalyst potential and work function values upon anodic polarization. The results are of significant practical importance and the exact underlying mechanism is worth further investigation.

Acknowledgement CGV expresses his warm thanks to Professor Christos Comninellis for many helpful discussions and for a fruitful and pleasant collaboration on the EPOC effect during the last 20 years.

References

1. Tauster SJ, Fung SC, Garten RL (1978) J Am Chem Soc 100:170
2. Resasco DE, Haller GL (1983) J Catal 82:279
3. Cairns JA, Baglin JE, Clark GL, Zeigler JF (1983) J Catal 83:301
4. Belton DN, Sun YM, White JM (1984) Phys Chem 88:1690
5. Ko CS, Gorte RJ (1984) J Catal 90:59
6. Tauster SJ (1987) Acc Chem Res 20:389
7. Haller JL, Resasco DE (1987) Adv Catal 36:173
8. Nicole J, Tsiplakides D, Pliangos C, Verykios XE, Comninellis Ch, Vayenas CG (2001) J Catal 204:23
9. Pliangos C, Yentekakis IV, Ladas S, Vayenas CG (1996) J Catal 159:189
10. Constantinou I, Archonta D, Brosda S, Lepage M, Sakamoto Y, Vayenas CG (2007) J Catal 251:400
11. Francioso L, Presicce DS, Taurino AM, Rella R, Siciliano P, Ficarella A (2003) Sens Actuat B 95:66
12. Sopyan I, Murasawa S, Hashimoto K, Fujishima A (1993) In: Ollis DE, Al Ekabi H (eds) Photocatalytic purification and treatment of water and air. Elsevier, Amsterdam
13. Ollis DE, Al-Ekabi H (eds) (1993) Proceedings of the 1st International Conference on TiO_2 Photocatalytic purification and treatment of water and air. Elsevier, Amsterdam, p 747
14. Fujishima A, Honda K (1972) Nature 238:37
15. Graetzel M (1991) Comments Inorg Chem 12:93
16. Watanabe T, Kitamura A, Kojima E, Nakayama C, Hashimoto K, Fujishima A (1994) Chem Lett 23:723
17. Battiston GA, Gerbasi R, Porchia M, Marigo A (1994) Thin Solid Films 239:186
18. Williams LM, Hess DW (1983) J Vac Sci Technol A1:1810
19. Fujii T, Sakata N, Takada J, Miura Y, Daitoh Y (1994) J Mater Res 9:1468
20. Vayenas CG, Bebelis S, Pliangos C, Brosda S, Tsiplakides D (2001) Electrochemical activation of catalysis: promotion electrochemical promotion and metal-support interactions. Kluwer Academic/Plenum Publishers, New York
21. Vayenas CG, Koutsodontis C (2008) J Chem Phys 128:182506
22. Vayenas GG, Bebelis S, Ladas S (1990) Nature 343:625
23. Anastasijevic NA, Baltruschat H, Heitbaum (1993) J Electrochim Acta 38:1067
24. Cavalca C, Larsen C, Vayenas CG, Haller GJ (1993) Phys Chem 97:6115
25. Pachioni G, Illas F, Neophytides S, Vayenas CG (1996) J Phys Chem 100:16553
26. Neophytides S, Tsiplakides D, Stonehart P, Jaksic M, Vayenas CG (1994) Nature (London) 370:292
27. Petrushina IM, Bandur VA, Cappeln F, Bjerrum NJ (2000) J Electrochem Soc 147:3010
28. Riess I, Vayenas CG (2003) Solid State Ionics 159:313
29. Jaccoud A, Falgairette C, Foti G, Comninellis Ch (2007) Electrochim Acta 52:7927
30. De Lucas-Consuegra A, Dorado F, Jimenez-Borja C, Valverde JL (2008) J Appl Electrochem 38:1151
31. Li X, Gaillard F, Vernoux P (2007) Top Catal 44:391
32. Leiva EPM, Vázquez C, Rojas MI, Mariscal MM (2008) J Appl Electrochem 38:1065
33. Balomenou SP, Tsiplakides D, Katsaounis A, Thiemann-Handler S, Cramer B, Foti G, Comninellis Ch, Vayenas CG (2004) Appl Catal B 52:181
34. Baranova EA, Fóti G, Comninellis Ch (2004) Electrochem Commun 6:170
35. Baranova EA, Fóti G, Comninellis Ch (2004) Electrochem Commun 6:389
36. Wüthrich R, Baranova EA, Bleuler H, Comninellis Ch (2004) Electrochem Commun 6:1199
37. Baranova EA, Thursfield A, Brosda S, Fóti G, Comninellis Ch, Vayenas CG (2005) J Electrochem Soc 152(2):E40
38. Baranova EA, Thursfield A, Brosda S, Foti G, Comninellis Ch, Vayenas CG (2005) Catal Lett 105(1–2):15
39. Papaioannou EI, Souentie S, Hammad A, Vayenas CG (2009) Catal Today 146:336
40. Lin H, Rumaiz AK, Schulz M, Wang D, Rock R, Huang CP, Shah SI (2008) Mater Sci Eng B 151:133
41. Hattori A, Tada H (2001) Sol-Gel Sci Technol 22:47
42. Harju M, Areva S, Rosenholm JB, Mäntylä T (2008) Appl Surf Sci 254:5981
43. Jensen H, Soloviev A, Li Z, Søgaard EG (2005) Appl Surf Sci 246:239
44. Spurr A, Myers H (1957) Anal Chem 59:761